

Relaxation Effects in a System of a Spin-1/2 Nucleus Coupled to a Quadrupolar Spin Subjected to RF Irradiation: Evaluation of Broadband Decoupling Schemes

Scott A. Smith and Nagarajan Murali¹

Center for Interdisciplinary Magnetic Resonance, National High Magnetic Field Laboratory, 1800 East Paul Dirac Drive, Tallahassee, Florida 32306-4005

Received May 28, 1998

We have investigated the suitability and performance of various decoupling methods on systems in which an observed spin-1/2 nucleus I (^{13}C or ^{15}N) is scalar-coupled to a quadrupolar spin S (^2H). Simulations and experiments have been conducted by varying the strength of the irradiating radiofrequency (RF) field, RF offset, relaxation times, and decoupling schemes applied in the vicinity of the S -spin resonance. The T_1 relaxation of the quadrupolar spin has previously been shown to influence the efficiency of continuous wave (CW) decoupling applied on resonance in such spin systems. Similarly, the performance of broadband decoupling sequences should also be affected by relaxation. However, virtually all of the more commonly used broadband decoupling schemes have been developed without consideration of relaxation effects. As a consequence, it is not obvious how one selects a suitable sequence for decoupling quadrupolar nuclei with exotic relaxation behavior. Herein we demonstrate that, despite its simplicity, WALTZ-16 decoupling is relatively robust under a wide range of conditions. In these systems it performs as well as the more recently developed decoupling schemes for wide bandwidth applications such as GARP-1 and CHIRP-95. It is suggested that in macromolecular motional regimes, broadband deuterium decoupling can be achieved with relatively low RF amplitudes (500–700 Hz) using WALTZ-16 multiple pulse decoupling. © 1999 Academic Press

Key Words: decoupling; relaxation; quadrupole relaxation; GAMMA; dynamic frequency shifts.

INTRODUCTION

NMR active isotope enrichment in biologically important macromolecules has opened new avenues for investigations into their solution structure (1, 2). Such enrichment is now frequently used to improve the information content in multidimensional NMR experiments. Long before the development of multidimensional NMR techniques, it had been realized that substitution of ^1H by ^2H would greatly diminish the dipolar relaxation of an attached ^{13}C or ^{15}N and narrow spectral linewidths of the latter nuclei (3). However, with increased molecular mass of systems under study and increased spectrometer field strengths, deuterium-quadrupole relaxation ef-

fects often counterbalance the latter benefit (3, 4). In macromolecular motional regimes the interference effects arising from the simultaneous presence of tensor interactions of the same rank (dipolar, quadrupolar, and shielding anisotropy) can cause observable dynamic frequency shifts (5), leading to asymmetric multiplet patterns. Furthermore the J -coupling interaction between the spin $I = 1/2$ nucleus and that of ^2H (spin S) is rendered time dependent by rapid quadrupolar relaxation, causing the splittings in the I spin spectrum to be either partially collapsed or totally washed-out, and is an additional source of line broadening for the spectrum of the spin-1/2 nucleus. It is highly desirable to minimize the latter relaxation effects by applying decoupling RF fields in the vicinity of the

TABLE 1
 ^{13}C Liouvillian Eigensystem of ^{13}C - ^2H and Intensities following a 90_y Pulse

τ_{sph} (ns)	Frequency (Hz)	Intensity	Phase (deg.)	Linewidth (Hz)
—	22.0	0.5	0.0	0.0
	0.0	0.5	0.0	0.0
	-22.0	0.5	0.0	0.0
0.1	21.727	0.502	15.021	8.749
	-0.020	0.530	0.028	5.766
	-21.717	0.502	-15.038	8.598
1.0	16.156	0.490	103.361	47.079
	-1.794	1.883	-3.408	24.310
	-14.704	0.451	-126.159	47.960
9.0	22.864	0.499	18.428	18.228
	-3.761	0.522	9.310	16.311
	-19.712	0.566	-25.324	10.187

Note. Simulated ^{13}C spectra of the ^{13}C - ^2H portion of glycerol- d_8 following a hard 90_y pulse. The values represent the Liouvillian eigensystem in accordance with Eqs. [3] and [4]. The three eigentransitions of the isotropic high-resolution NMR Hamiltonian (equal to the top spectrum, without relaxation) blend to form three eigenfrequencies of the Liouvillian under BWR relaxation. When formed into Lorentzians, this discrete information produces the three spectra of Fig. 1, middle column.

¹ To whom correspondence should be addressed.

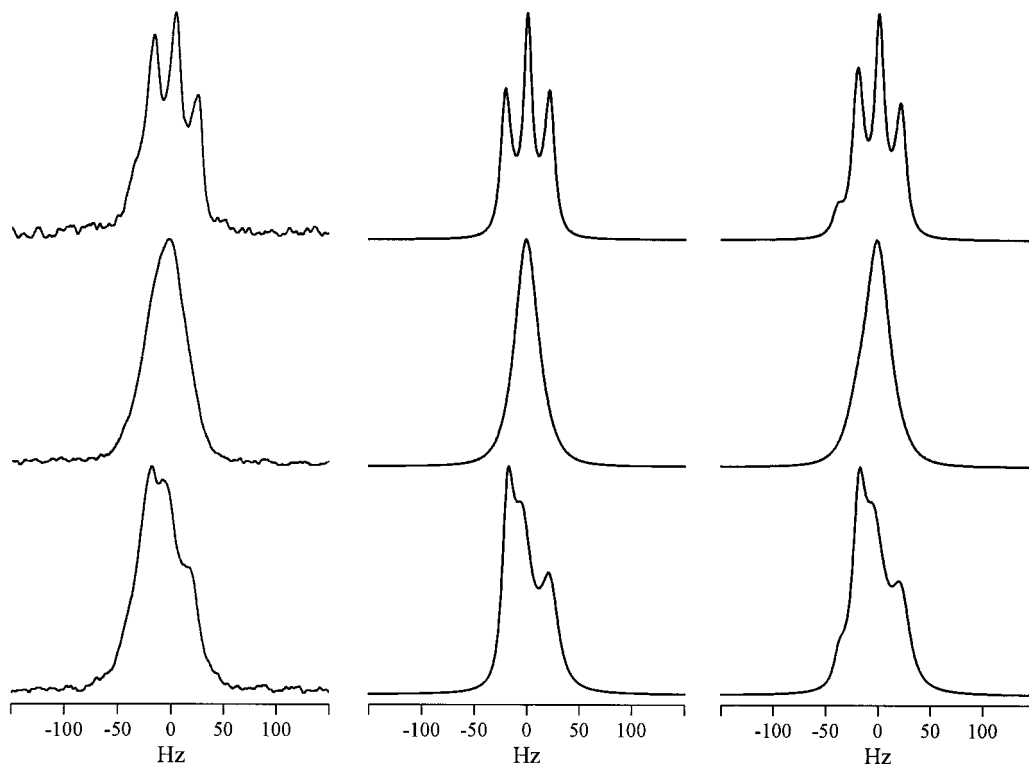


FIG. 1. 180 MHz ^{13}C spectra (720 MHz ^1H) of the ^{13}C - ^2H portion of glycerol- d_8 in DMSO- d_6 . Left column: Experimental spectra recorded at sample temperatures of 24°C, -10°C, and -45°C top to bottom. The spectral width was set to 11,500.9 Hz and 16K points taken per temperature. The data were zero filled to 64K and a 2.0 Hz line broadening was applied prior to Fourier transformation. Middle column: GAMMA simulated spectra using spherical rotational correlation times of 0.1, 1.0, and 9.0 ns top to bottom. The spectral width was set to 300 Hz and 512 FID points were calculated per correlation time. A 2.0 Hz line broadening was applied prior to Fourier transformation. Right column: GAMMA simulated spectra matching the middle column but including a 20% impurity detected in the experimental sample. Additional simulation parameters were $J(^{13}\text{C}-^2\text{H}) = 22$ Hz, $r(^{13}\text{C}-^2\text{H}) = 1.09$ Å, $\text{CSA}(^{13}\text{C}) = 100$ ppm, $\text{QCC}(^2\text{H}) = 175$ kHz. For simplicity the dipolar, quadrupolar, and shift anisotropy principal axes were set coincident and their asymmetry values set to zero. Although their relative orientations do affect the lineshapes, they had little effect on the simulated decoupling profiles in Figs. 4, 5, and 7.

S-spin resonances. A rigorous theoretical treatment of a two-spin system detailed how the spin-1/2 transition linewidths, positions, and intensities are affected by CW irradiation on the spin-1 nucleus (6). The predicted spectral changes can be dramatic and very much depend on both the RF-field strength and the inherent spin system relaxation pathways.

Our current motivation is to arrive at an optimal ^2H decoupling strategy in macromolecular motional regimes. In order to cover the entire deuterium spectral range under modest RF amplitudes, employment of broadband techniques will be required. Almost all the commonly used broadband decoupling schemes have been developed without consideration of relaxation effects. Accordingly, it is not straightforward to select a suitable broadband scheme for decoupling quadrupolar nuclei with relatively exotic relaxation behavior. Many of the multiple-pulse sequences have been based on applying cycles of RF pulse elements, each element a composite inversion pulse that has uniform inversion with respect to offsets. In turn, it is tacitly assumed that the spectrum of the decoupled spins appears as well resolved lines. It is not clear whether such

schemes would perform well when the decoupled spins are influenced by rapid quadrupolar relaxation leading to much broader lines. Although more recent schemes such as GARP-1 do not invoke such a criterion (uniform inversion) and explicitly treat the coupling part of the Hamiltonian, the effects of relaxation on such a sequence is unknown.

Extending our earlier work on CW decoupling (6), we have investigated relaxation effects with respect to the various broadband decoupling schemes. An analytical treatment of broadband decoupling, including relaxation dynamics, would be a formidable task. We approached the problem of theoretically evaluating the various schemes under different relaxation conditions using the GAMMA simulation platform (7). The calculations use an exact theoretical treatment based on the solution of the complete density matrix equations, including both coherent and incoherent parts of the spin Hamiltonian. The simulations are compared with decoupling experiments that have been conducted on a perdeuterated glycerol sample in a DMSO- d_6 /D $_2$ O solvent mixture using a Varian Unity Plus 720 MHz spectrometer. The reason for choosing this particular

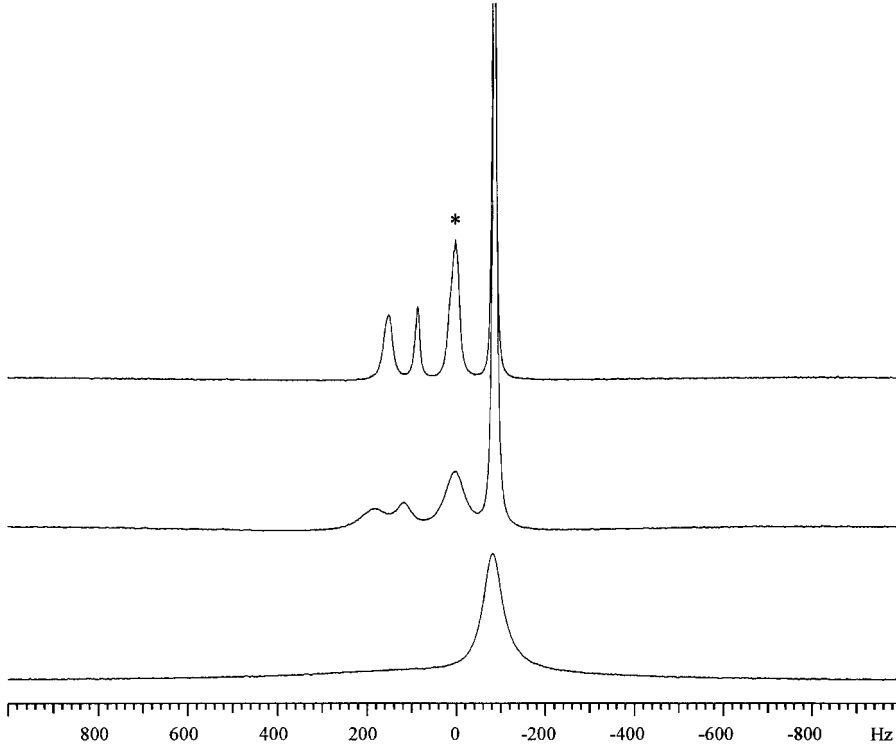


FIG. 2. Deuterium spectra of glycerol-*d*8 in DMSO-*d*6 recorded at various temperatures. The ^2H frequency was 110 MHz.

sample, as previously reported (8, 9), is that the viscosity of the glycerol molecule could be varied by changing the sample temperature, which in turn allowed us to probe a wide range of motional regimes with different rotational correlation times and relaxation rates.

THEORY

Computation of spectra can be based on evaluation of the expectation value of the observable in the density operator equations

$$\langle O \rangle = \langle O^\dagger | \sigma \rangle,$$

$$|\sigma(t)\rangle = e^{-i\hat{L}t} |\sigma_o - \sigma_\infty\rangle + |\sigma_\infty\rangle = e^{-i\hat{L}t} |\Delta\sigma_o\rangle + |\sigma_\infty\rangle. \quad [1]$$

Here, the density operator $|\sigma\rangle$ is evolved under the superoperator Liouvillian \hat{L} and O is any operator associated with a quantity whose expectation value is $\langle O \rangle$. Given a system which has been prepared by some arbitrary pulse sequence, $|\sigma_p\rangle$, an FID in NMR would be formally given by

$$\text{FID}(t) = \langle F_-^\dagger | e^{-i\hat{L}t} |\Delta\sigma_p\rangle + \langle F_-^\dagger | \sigma_\infty \rangle. \quad [2]$$

The GAMMA platform contains operators and superoperators as abstract data types, and has an implementation of the analog

Fourier transform of Eq. [2] in order to generate frequency domain spectra directly. Using the eigensystem of the Liouvillian, $\hat{L} = \hat{S}\hat{\Lambda}\hat{S}^{-1}$, and defining the constant $K = \langle F_-^\dagger | \sigma_\infty \rangle$, one obtains the FID as

$$\text{FID}(t) = \langle F_-^\dagger | \hat{S} | e^{-i\hat{\Lambda}t} | \hat{S}^{-1} \Delta\sigma_p \rangle + K, \quad [3]$$

and the spectrum as

$$\begin{aligned} S(\omega) &= \int_0^\infty \text{FID}(t) e^{-i\omega t} dt \\ &= \left\langle F_-^\dagger | \hat{S} \left| \left(\int_0^\infty e^{-i\hat{\Lambda}t} e^{-i\omega t} dt \right) \right| \hat{S}^{-1} \sigma_p - \sigma_\infty \right\rangle \\ &\quad + K \int_0^\infty e^{-i\omega t} dt. \end{aligned} \quad [4]$$

Without an applied RF field during an acquisition the infinite time density operator is just the equilibrium density operator, $\sigma_\infty = \sigma_{eq}$, which does not contribute to transverse magnetization, and K is zero. If there is an applied field during the

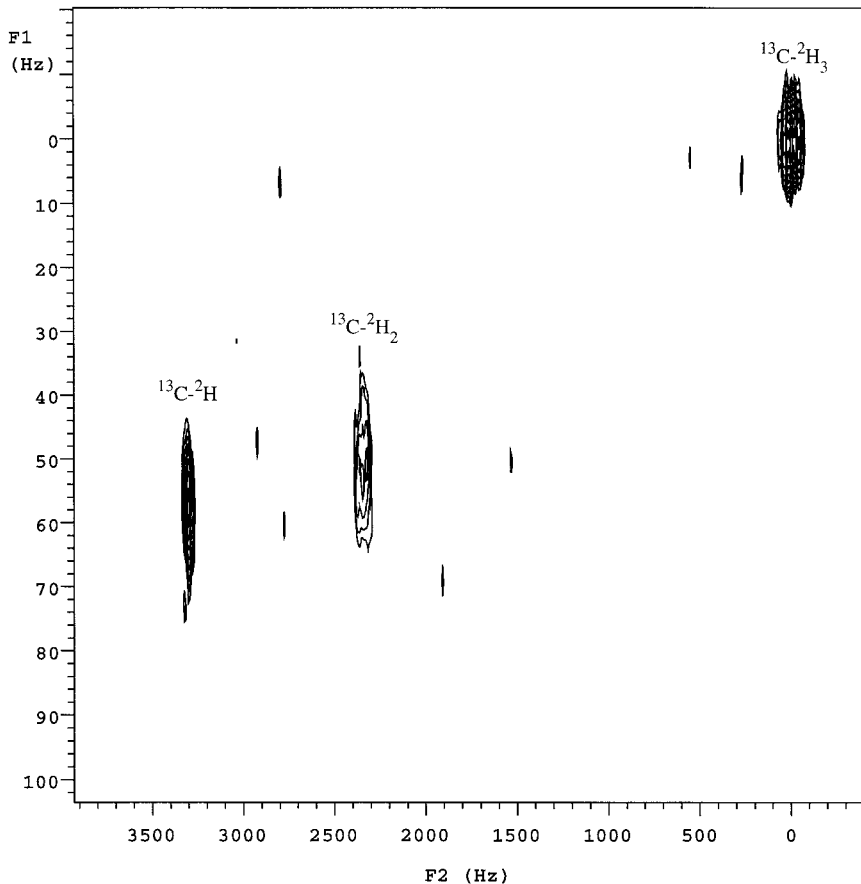


FIG. 3. ^2H - ^{13}C HMQC spectrum of the glycerol- d_8 in DMSO- d_6 recorded at room temperature using a Varian Inova 400 MHz spectrometer. The Larmor frequencies of ^{13}C and ^2H were 100.573 and 61.395 MHz, respectively. The carbon spectral width (F_2) was 5798.4 Hz and the deuterium spectral width (F_1) was 800 Hz. The time domain data were recorded using the States method, yielding 128×2048 data points, and the phase sensitive spectrum is obtained after zero filling to 1024×2048 data points prior to the 2D FFT.

acquisition, K usually represents a spike in the spectrum at the RF-field frequency.

The more interesting aspect of Eq. [4] is the part which involves the Liouvillian eigensystem. The eigenvalues of $\hat{\mathcal{L}}$ (elements of $\hat{\Lambda}$, λ_i) are complex numbers and, when detected (by F_-), contribute oscillating exponentially decaying terms to the FID. The imaginary part of each λ_i is an eigenfrequency that is a linear combination of the isotropic Hamiltonian transitions. This concept is analogous to the way strong coupling alters observed transition frequencies in high-resolution spectra, irrespective of relaxation. With strong relaxation, it is the transitions (rather than the energy levels) that blend and, because the full Liouvillian is complex, their intensities may be complex as well. Subsequent Fourier transformation of the decaying eigenfrequencies produces Lorentzians with particular offsets, linewidths, and *phases* that contribute to the frequency spectrum. This is readily seen in Table 1, which contains a listing of λ_i values for the system being studied, along with their associated intensities (a product of $\langle F_-^\dagger \hat{S} \rangle$ and $|\hat{S}^{-1} \Delta \sigma_p\rangle$ elements).

When a broadband decoupling sequence is applied, for each new step of duration Δt in the decoupling sequence the density operator is evolved from the state of the operator of the previous step according to Eq. [1],

$$|\sigma_i(t)\rangle = e^{-i\hat{\mathcal{L}}_i \Delta t} |\sigma_{i-1}(t) - \sigma_{i,\infty}\rangle + |\sigma_{i,\infty}\rangle. \quad [5]$$

It is extremely tedious to evolve the system through such a sequence because the active Hamiltonian, step length, and steady-state density operator may be constantly changing. The difficulty is compounded by the need to sample FID points at even increments, yet allow for any arbitrary waveform during decoupling. Making use of superoperator propagators (10) which allow Eq. [1] to be rewritten as

$$|\sigma(t)\rangle = \hat{\Gamma}(t) |\sigma_o\rangle, \quad [6]$$

one can easily construct multistep propagators while still rigorously accounting for relaxation and exchange effects. This

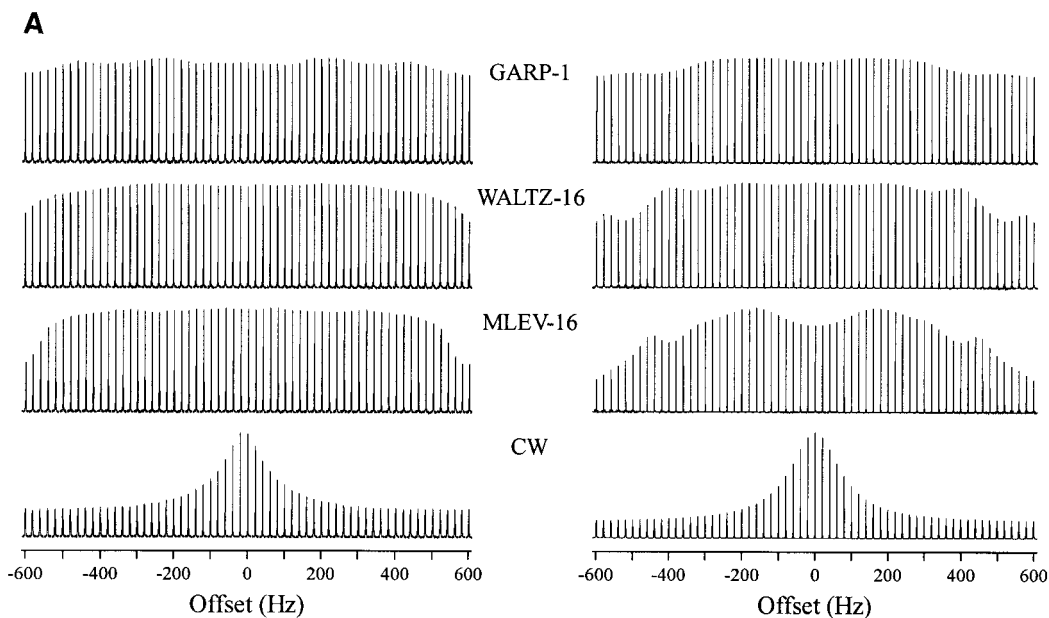


FIG. 4. Experimental (left column) and simulated (right column) 180 MHz ^{13}C spectra of the ^{13}C - ^2H portion of glycerol- d_8 versus ^2H decoupler offset. The decoupler RF amplitude was set at $\gamma B_1 = 435$ Hz. A total of 61 offsets were taken in increments of 20 Hz. The plotted range on each was 300 Hz centered about the ^{13}C shift. Experimental: The spectral width was set to 11,500.9 Hz and 16K points taken per offset. The data were zero filled to 64K and a 2.0 Hz line broadening was applied prior to Fourier transformation. Simulation: Spin system parameters used in the simulations match those used in Fig. 1 except as noted. The experimental sample temperatures and simulation correlation times are (A) 24°C, 0.1 ns; (B) -10°C, 1.0 ns; (C) -45°C, 9.0 ns.

has been implemented in the GAMMA platform, which now readily allows for simulations of both complex mixing sequences and acquisitions during decoupling.

EXPERIMENTS AND SIMULATIONS

All experiments were performed on a solution containing perdeuterated glycerol. The solvent was DMSO- d_6 to which a small amount of a sugar (amylose dissolved in D_2O) was added. This mixture prevented the sample from freezing at low temperatures. The experiments were carried out using a Varian Unity plus 720 MHz spectrometer.

The ability of the glycerol molecule to mimic various motional regimes is best illustrated in the experimental spectra recorded as a function of temperature (Fig. 1, left column). Similar experiments were also reported earlier by Grzesiek and Bax (9). The lineshape of the ^{13}C multiplets (in the absence of decoupling) arising from the ^{13}C - ^2H group shows a triplet at a temperature 24°C and corresponds to a small molecule motional regime. The multiplet structure initially began to collapse as the temperature was lowered further and the spectrum recorded at -10°C appears as a broad singlet. The observed linewidth in this spectrum has additional contributions from scalar relaxation of the second kind. At even colder temperatures some structure reappears, and the asymmetric triplet at -45°C clearly exhibits cross-correlation effects. Dynamic frequency shifts predominantly arise from the cross correlation

between the ^{13}C - ^2H dipolar and ^2H quadrupolar interactions. Differential linewidths are caused from the cross correlation between ^{13}C - ^2H dipolar and ^{13}C shift anisotropy interactions (see Table 1). These carbon spectra provide a basis for making quick estimations of system dynamics versus temperature when compared to simulated lineshapes. The center column in Fig. 1 contains spectra simulated by GAMMA for various rotational correlation times under rigid spherical top diffusional dynamics using a BWR treatment of relaxation (11). The correlation times, top to bottom, are 0.1, 1.0, and 9.0 ns, respectively, and roughly coincide with the dynamics exhibited in the experimental spectra. The simulated spectra in the right-most column in Fig. 1 are a repeat of center column calculations except that they include a 20% impurity which has a ^{13}C (coupled to deuterium), yielding a similar spectrum shifted by about -17 Hz. The impurity peak appears as a completely resolved singlet at 24°C under complete deuterium decoupling. Much of the asymmetry in the experimental spectra at 24°C is due to this impurity, not dipole-CSA cross correlation as one might suspect.

In Fig. 2 the deuterium spectra of the glycerol sample recorded at various temperatures are presented. The peak (marked by an asterisk) next to the sharp intense solvent signal arises from the deuterons in both the ^{13}C - ^2H and ^{13}C - $^2\text{H}_2$ groups of glycerol. The resonance assignments were confirmed by the ^{13}C - ^2H HMQC experiment (Fig. 3) so that the decou-

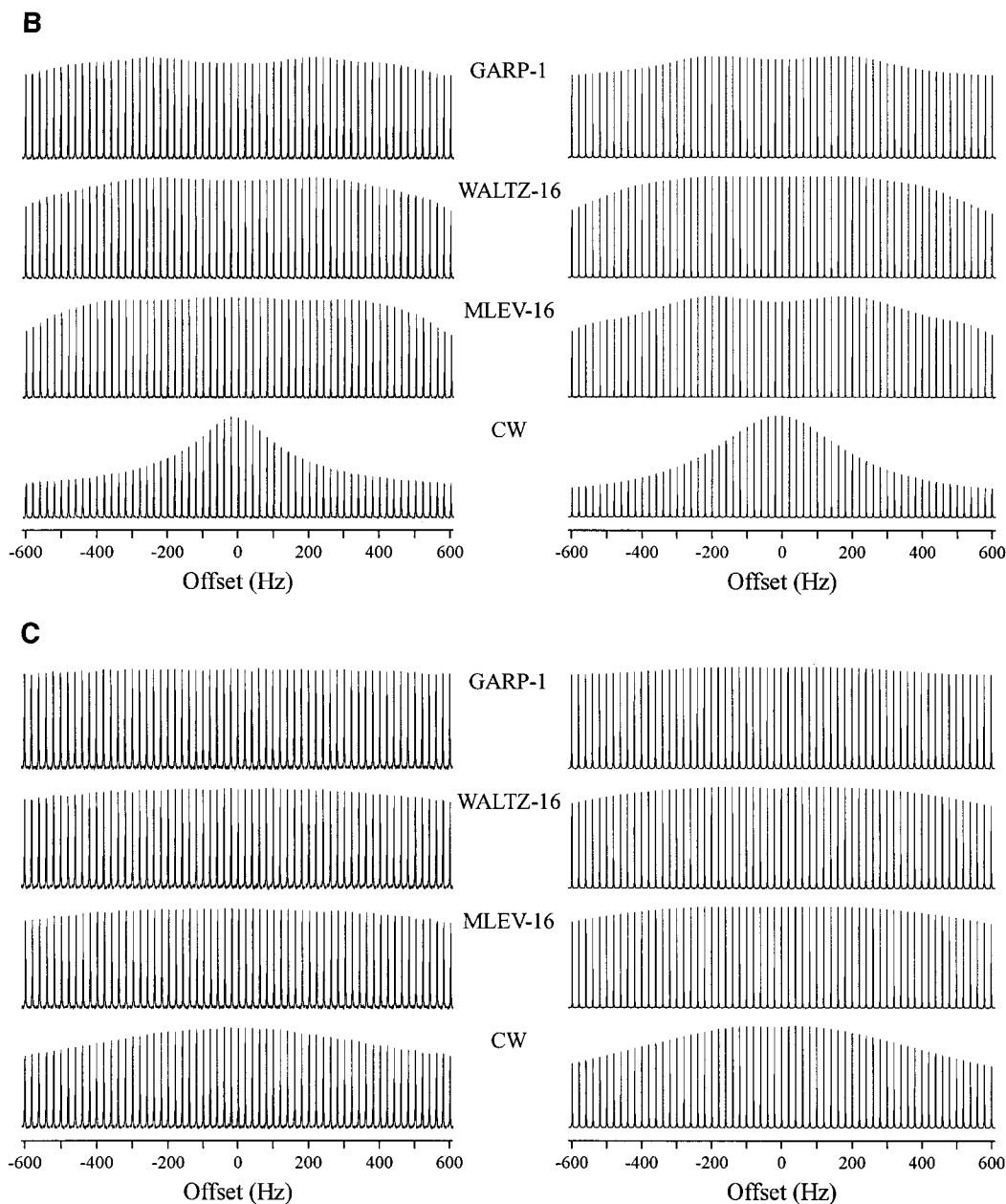


FIG. 4—Continued

pler offsets can be specifically set relative to the deuterium resonance of the glycerol ^{13}C - ^2H . It should be noted that the ^2H resonances also broaden as the temperature is lowered due to the decrease in its quadrupolar T_2 , and at -45°C the resonances from glycerol are so broad as to be unobservable. In contrast, the corresponding ^{13}C spectrum shows an asymmetric triplet since carbon is only affected by the relatively weaker dipolar relaxation and the effects of the ^2H quadrupole relaxation appear only through cross correlation.

From the simulations in Fig. 1, we estimate that the quadrupolar T_{1Q} is on the order of 22 ms at 24°C , about 5 ms at

-10°C , and around 24 ms at -45°C . It has been shown (6) that for complete CW decoupling the condition

$$\omega_r J^{-1} \gg 1 \quad [7]$$

must be satisfied and that in order to suppress scalar relaxation of the second kind the condition

$$\omega_r T_{1Q} \gg 1 \quad [8]$$

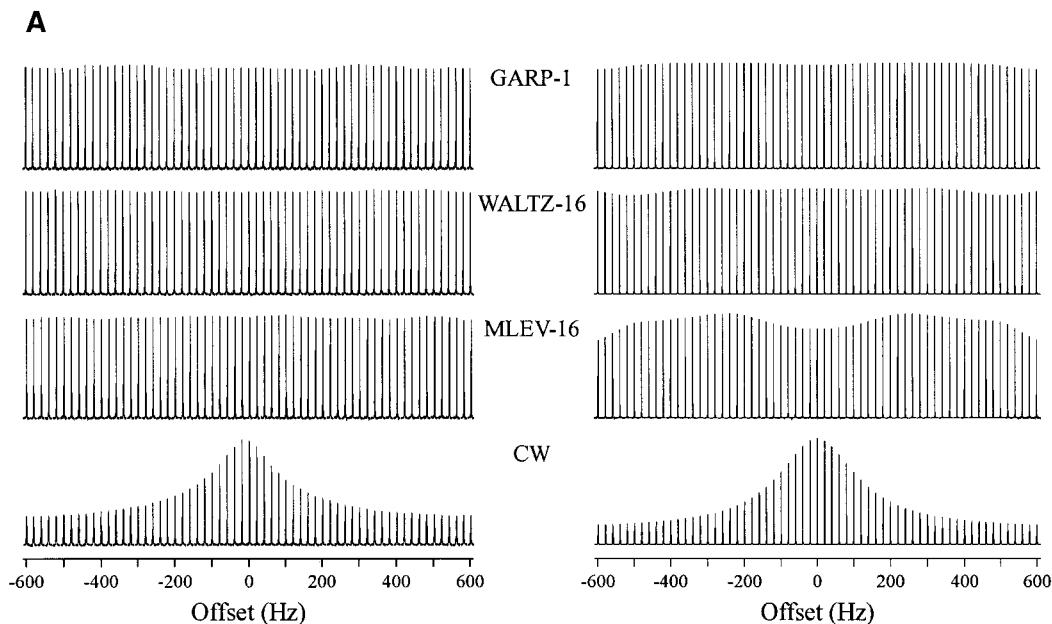


FIG. 5. Experimental (left column) and simulated (right column) 180 MHz ^{13}C spectra of the ^{13}C - ^2H portion of glycerol- d_8 versus ^2H decoupler offset. The decoupler RF amplitude was set at $\gamma B_1 = 686$ Hz. All other parameters were identical to those specified in Fig. 4.

should be met. In these equations ω_r is the RF amplitude applied at on resonance, J is the scalar coupling, and T_{1Q} is the longitudinal relaxation time of the quadrupolar nucleus. For the methyne carbon of glycerol, the ^{13}C - ^2H scalar coupling is about $J/(2\pi) = 22$ Hz, $((J/(2\pi))^{-1} \sim 45$ ms). It is therefore reasonable to use RF amplitudes over 400 Hz for quadrupolar spin decoupling since this also satisfies Eq. [8] even for the shortest T_{1Q} (5 ms). However, it is not obvious that such an RF amplitude level would be sufficient for broadband decoupling, especially in situations at low temperatures when the deuterium resonance is completely broadened. Decoupling schemes such as MLEV-16 (12–15) and WALTZ-16 (16–18) have been developed by satisfying the requirement of complete inversion of the resonances of the decoupled nuclei over a wide range of offsets. It appears that these and other multiple pulse schemes would require formidably high RF amplitudes for decoupling deuterium in the present sample at low temperatures.

In order to evaluate the efficiency of various decoupling methods a series of experiments and simulations was carried out with ^2H decoupling during acquisition. The experiments (Figs. 4 and 5, left column) were performed at three temperatures (as in Fig. 1, left column) and the simulations (Figs. 4 and 5, right column) run with matching rotational correlation times (as in Fig. 1, center column). The decoupling schemes applied were continuous wave (CW), MLEV-16, WALTZ-16, GARP-1 (19), and CHIRP-95 (20). These were repeated with the decoupling RF amplitude levels set at 435 Hz (Fig. 4) and 686 Hz (Fig. 5). The deuterium decoupling offset was varied in a range +600 to -600 Hz (corresponding to about +6 to -6 ppm at $\nu_0(^2\text{H}) = 110$ MHz) in steps of 20 Hz from the

on-resonance position. Both experiments and calculations using the multiple pulse decoupling methods required asynchronous acquisitions; i.e., the dwell time as dictated by the desired spectral width does not match the decoupling cycle length. Simulations (not shown) comparing synchronous to asynchronous acquisitions indicate significant differences in decoupler performance. The asynchronous case typically produces baseline instabilities and a multitude of overtone frequencies, present in both experimental and simulated spectra in these two figures.

To evaluate ultra-broadband decoupling, experimental spectra under CHIRP-95 decoupling (20) set at the two RF levels are presented in Fig. 6. Finally, to detail the effects of relaxation, profiles were simulated without relaxation (Fig. 7, left column) and with relaxation but without cross-correlation effects (Fig. 7, right column).

CONCLUSION

Using both experiments and simulations it has been demonstrated that relatively low RF amplitudes are sufficient to decouple deuterium even over a wide range of offsets. The performance of the various decoupling schemes depends upon the relaxation rates involved, as is evident from spectra recorded as a function of temperature. At temperatures of 24°C and -10°C, wherein the deuterium spectra from the glycerol molecule show well-defined resonances (Fig. 2), the decoupling bandwidth improves as the RF amplitude is increased to 686 Hz in accordance with Eq. [7]. At -45°C, with an even shorter deuterium T_2 , not only the various broadband schemes,

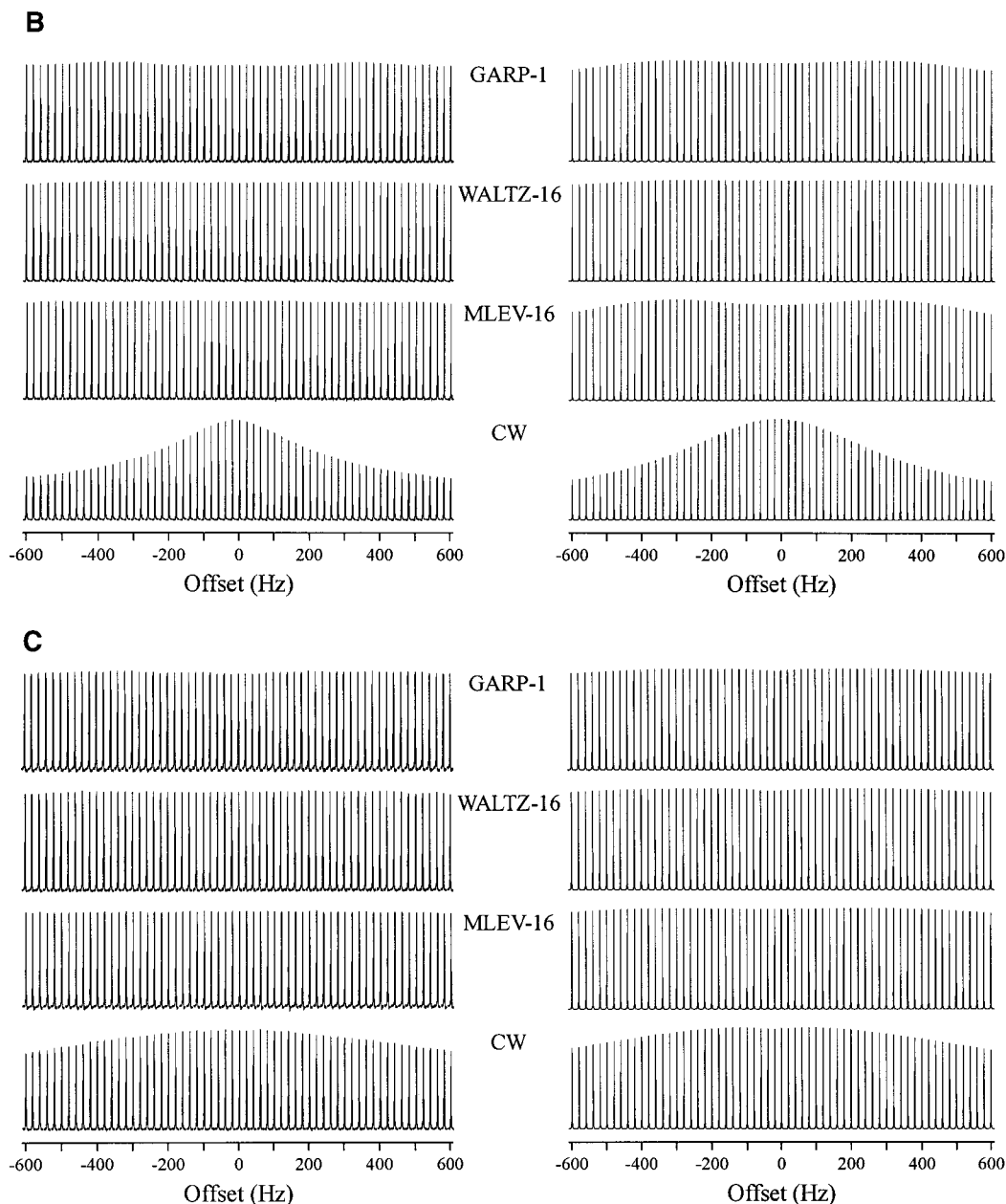


FIG. 5—Continued

but also CW decoupling, perform reasonably well even at the lower RF amplitude of 435 Hz. This suggests that these decoupling approaches can well be applied with modest levels of RF amplitude to systems having broad resonances.

The superior performances of WALTZ-16 and MLEV-16 at the lowest temperature appear to be in contradiction to intuition, as these broadband decoupling sequences are designed on the basis of the inversion profile of sharp resonances. Inversion of such a broad (unobservable) resonance line implies that a formidable level of RF amplitude would be required. The experiments and simulations presented here indi-

cate that, in the case of broad resonances, it is reasonable to think in terms of the frequency spectrum of the decoupling profile as a deciding factor for decoupling bandwidth efficiency rather than the optimal performance of inversion over a frequency range.

A rationale for efficient decoupling observed at -45°C is that at larger offsets the trailing tail of the broad deuterium resonance still becomes irradiated, leading to the multiplet collapse in the carbon spectrum. It is worth noting that the performance of CW decoupling is also improved over a wider bandwidth for this same reason. This is further verified by

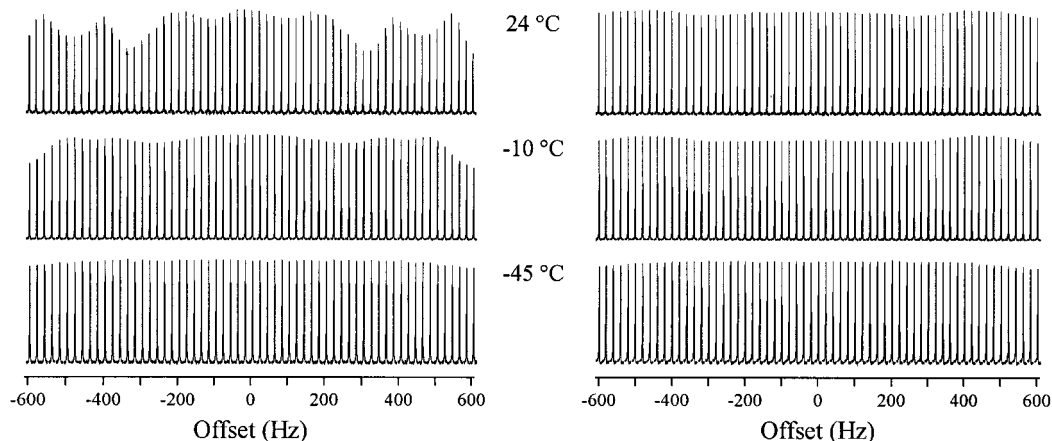


FIG. 6. Experimental 180 MHz ^{13}C spectra of the ^{13}C - ^2H portion of glycerol- d_8 under CHIRP-95 decoupling. In the left column, $\gamma B_1 = 435$ Hz, the $\Delta\nu$ (sweep) = 1 kHz, and a PW = 1 ms was used for the spectra at 24°C, and for the other two temperatures $\Delta\nu$ (sweep) = 0.7 kHz and PW = 1 ms. In the right column, $\gamma B_1 = 686$ Hz, the $\Delta\nu$ (sweep) = 1 kHz, and a PW = 1 ms was used for the spectra at 24°C, and for the other two temperatures $\Delta\nu$ (sweep) = 0.8 kHz and PW = 1 ms (16).

profile simulations without relaxation (Fig. 7, *left*) wherein CW, MLEV-16, and WALTZ-16 schemes show significant offset dependence when the RF amplitude is set at 435 Hz. Relaxation of the quadrupolar nucleus in fact *aids* the decoupler efficiency of these schemes, as seen from comparison with Fig. 4. In contrast, the strong cross correlation in this system has little influence in the decoupling profile, as seen by comparison of Fig. 7 (right) with Fig. 4.

It appears that the condition $\omega_r^2 T_{1Q} T_{2Q} \gg 1$ (which is also the condition for the saturation of spin S) as given in theoret-

ical descriptions of decoupling of quadrupolar spins and for suppressing scalar relaxation of the second kind in earlier literatures (3, 21) is rather unnecessary (6, 22). The relevant and sufficient conditions for decoupling and suppression of the scalar relaxation of the second kind are those given by Eqs. [7] and [8]. It should be stressed that in macromolecular motional regimes the condition $\omega_r^2 T_{1Q}^2 \gg 1$ is much more easily satisfied because $T_{1Q} > T_{2Q}$, and this suggests that use of a much lower RF amplitude is adequate compared to that given by the saturation condition. This difference has significant impact in op-

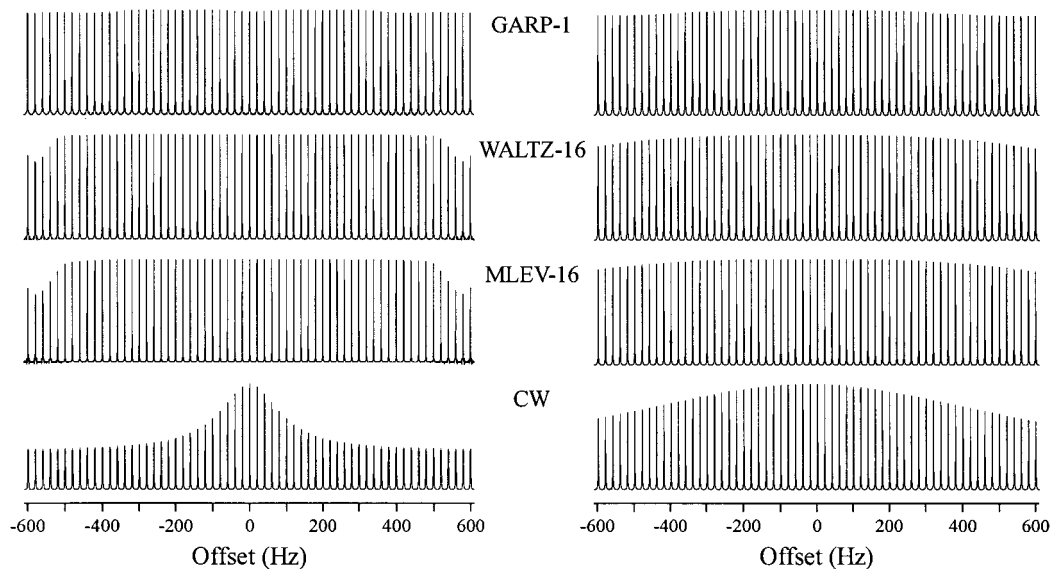


FIG. 7. Simulated 180 MHz ^{13}C spectra of the ^{13}C - ^2H portion of glycerol- d_8 . All parameters were identical to those in Fig. 4 at -45°C except as noted. *Left:* Without relaxation effects, an apodization of 10 Hz was used to match the linewidths in Fig. 4C. *Right:* Without dipole-quadrupole and dipole-CSA cross-correlation effects.

timizing RF field strengths when decoupling quadrupolar spins.

This work indicates that broadband schemes such as GARP-1 and CHIRP-95, developed for wider bandwidth applications, can be used effectively for deuterium decoupling. However, WALTZ-16 decoupling with RF amplitudes of $\gamma B_1/2\pi \sim 500\text{--}700$ Hz would be a superior choice, considering its effectiveness and relative ease of implementation along with the relatively small deuterium spectral range over which decoupling must be effective.

ACKNOWLEDGMENTS

Philippe Pelupessy is a co-author of the GAMMA pulse train modules used in preliminary decoupling simulations. Acknowledgments are due to the National High Magnetic Field Laboratory (NHMFL) for the use of the Varian Unity plus 720 MHz and support for GAMMA as part of the Center for Interdisciplinary Magnetic Resonance (CIMAR). For GAMMA information see <http://gamma.magnet.fsu.edu/>. Much of this work was presented in a poster at the ENC in Orlando, Florida, 1997. The GAMMA programs used herein, some of which may be interactively run at the WWW site, are available upon request.

REFERENCES

1. G. Wagner, *Prog. NMR. Spectrosc.* **22**, 101 (1990).
2. S. W. Fesik and E. R. P. Zuiderweg, *Q. Rev. Biophys.* **23**, 97 (1990).
3. D. T. Browne, G. L. Kenyon, E. L. Packer, H. Sternlicht, and D. M. Wilson, *J. Am. Chem. Soc.* **95**, 1316 (1972).
4. S. Grzesiek, J. Angaliester, H. Ren, and Ad Bax, *J. Am. Chem. Soc.* **115**, 4369 (1993).
5. R. E. London, D. M. LeMaster, and L. G. Werbelow, *J. Am. Chem. Soc.* **116**, 8400 (1994).
6. N. Murali and B. D. Nageswara Rao, *J. Magn. Reson. A* **118**, 202 (1996).
7. S. Smith, T. O. Levante, B. H. Meier, and R. R. Ernst, *J. Magn. Reson. A* **106**, 75 (1994).
8. B. D. Nageswara Rao and B. D. Ray, *J. Am. Chem. Soc.* **114**, 1566 (1992).
9. S. Grzesiek and A. Bax, *J. Am. Chem. Soc.* **116**, 10196 (1994).
10. S. Smith, W. E. Palke, and J. T. Gerig, *J. Magn. Reson. A* **106**, 57 (1994).
11. R. K. Wangsness and F. Bloch, *Phys. Rev.* **89**, 728 (1953); F. Bloch, *Phys. Rev.* **102**, 104 (1956); A. G. Redfield, *IBM J. Res. Develop.* **1**, 19 (1957).
12. M. H. Levitt and R. Freeman, *J. Magn. Reson.* **43**, 502 (1981).
13. M. H. Levitt, R. Freeman, and T. Frenkiel, *J. Magn. Reson.* **47**, 328 (1982).
14. M. H. Levitt, R. Freeman, and T. Frenkiel, *J. Magn. Reson.* **50**, 157 (1982).
15. M. H. Levitt, R. Freeman, and T. Frenkiel, in "Advances in Magnetic Resonance" (J. S. Waugh, Ed.), Vol. 12, p. 47, Academic Press, New York, 1982.
16. A. J. Shaka, J. Keeler, T. Frenkiel, and R. Freeman, *J. Magn. Reson.* **52**, 335 (1983).
17. A. J. Shaka, J. Keeler, and R. Freeman, *J. Magn. Reson.* **53**, 313 (1983).
18. A. J. Shaka and J. Keeler, *Prog. NMR Spectrosc.* **19**, 47 (1987).
19. A. J. Shaka, P. B. Barker, and R. Freeman, *J. Magn. Reson.* **64**, 547 (1985).
20. R. Fu and G. Bodenhausen, *J. Magn. Reson. A* **117**, 324 (1995).
21. N. R. Skrynnikov, S. F. Lienin, R. Bruschweiler, and R. R. Ernst, *J. Chem. Phys.* **108**, 7662 (1998).
22. A. Abragam, in "The Principles of Nuclear Magnetism," Chap. XII, p. 530, Clarendon Press, Oxford/London (1961).